RESEARCH/REVIEW ARTICLE

A quantitative x-ray diffraction inventory of volcaniclastic inputs into the marine sediment archives off Iceland: a contribution to the Volcanoes in the Arctic System programme

John T. Andrews,[1] Greta B. Kristjánsdóttir,[1,2] Dennis D. Eberl[3] & Anne E. Jennings[1]

[1] Department of Geological Sciences, Institute of Arctic and Alpine Research, University of Colorado, PO Box 450, Boulder, CO 80309, USA
[2] School of Engineering and Natural Sciences, University of Iceland, VR-II, Hjardarhaga 2-6, IS-107 Reykjavík, Iceland
[3] US Geological Survey, 3215 Marine St., Suite E-127, Boulder, CO 80303, USA

Keywords
X-ray diffraction; tephras; Iceland Holocene.

Correspondence
John T. Andrews, Department of Geological Sciences, Institute of Arctic and Alpine Research, University of Colorado, PO Box 450, Boulder, CO 80309, USA.
E-mail: andrewsj@colorado.edu

Abstract

This paper re-evaluates how well quantitative x-ray diffraction (qXRD) can be used as an exploratory method of the weight percentage (wt%) of volcaniclastic sediment, and to identify tephra events in marine cores. In the widely used RockJock v6 software programme, qXRD tephra and glass standards include the rhyodacite White River tephra (Alaska), a rhyolitic tephra (Hekla-4) and the basaltic Saksunarvatn tephra. Experiments of adding known wt% of tephra to felsic bedrock samples indicated that additions $\geq$10 wt% are accurately detected, but reliable estimates of lesser amounts are masked by amorphous material produced by milling. Volcaniclastic inputs range between 20 and 50 wt%. Primary tephra events are identified as peaks in residual qXRD glass wt% from fourth-order polynomial fits. In cores where tephras have been identified by shard counts in the >150 μm fraction, there is a positive correlation (validation) with peaks in the wt% glass estimated by qXRD. Geochemistry of tephra shards confirms the presence of several Hekla-sourced tephras in cores B997-317PC1 and -319PC2 on the northern Iceland shelf. In core B997-338 (north-west Iceland), there are two rhyolitic tephras separated by ca. 100 cm with uncorrected radiocarbon dates on articulated shells of around 13 000 yr B.P. These tephras may be correlatives of the Borrobol and Penifiler tephras found in Scotland. The number of Holocene tephra events per 1000 yr was estimated from qXRD on 16 cores and showed a bimodal distribution with an increased number of events in both the late and early Holocene.

To access the supplementary material for this article, please see the supplementary files under Article Tools online.

The Volcanoes in the Arctic System (VAST) programme is an international programme involving researchers in Iceland, Norway, the UK and the USA with goals of: (1) using tephras to integrate paleoclimate records by providing reliable isochrones, primarily within the Holocene; and (2) investigating the importance of high-latitude volcanic eruptions on the climate system (Kelly 1977; Oman et al. 2005; Zhong et al. 2011). Iceland, Alaska and Jan Mayen Island contributed to Holocene volcanic eruptions, but this paper focuses solely on Iceland (Fig. 1a). We present an inventory of volcaniclastic (i.e., reworked) sediments in the Holocene marine sediment archives around Iceland and, more fundamentally, attempt to present a preliminary inventory of probable primary tephra events. This paper is a companion paper to the compilation by Larsen & Eiríksson (2008), using the standard sieving and shard counting method, which gave the Holocene variability of Icelandic

Polar Research 2013. © 2013 J.T. Andrews et al. This is an open-access article distributed under the terms of the Creative Commons Attribution-Noncommercial 3.0 Unported License (http://creativecommons.org/licenses/by-nc/3.0/), permitting all non-commercial use, distribution, and reproduction in any medium, provided the original work is properly cited.
Citation: *Polar Research* 2013, *32*, 11130, http://dx.doi.org/10.3402/polar.v32i0.11130

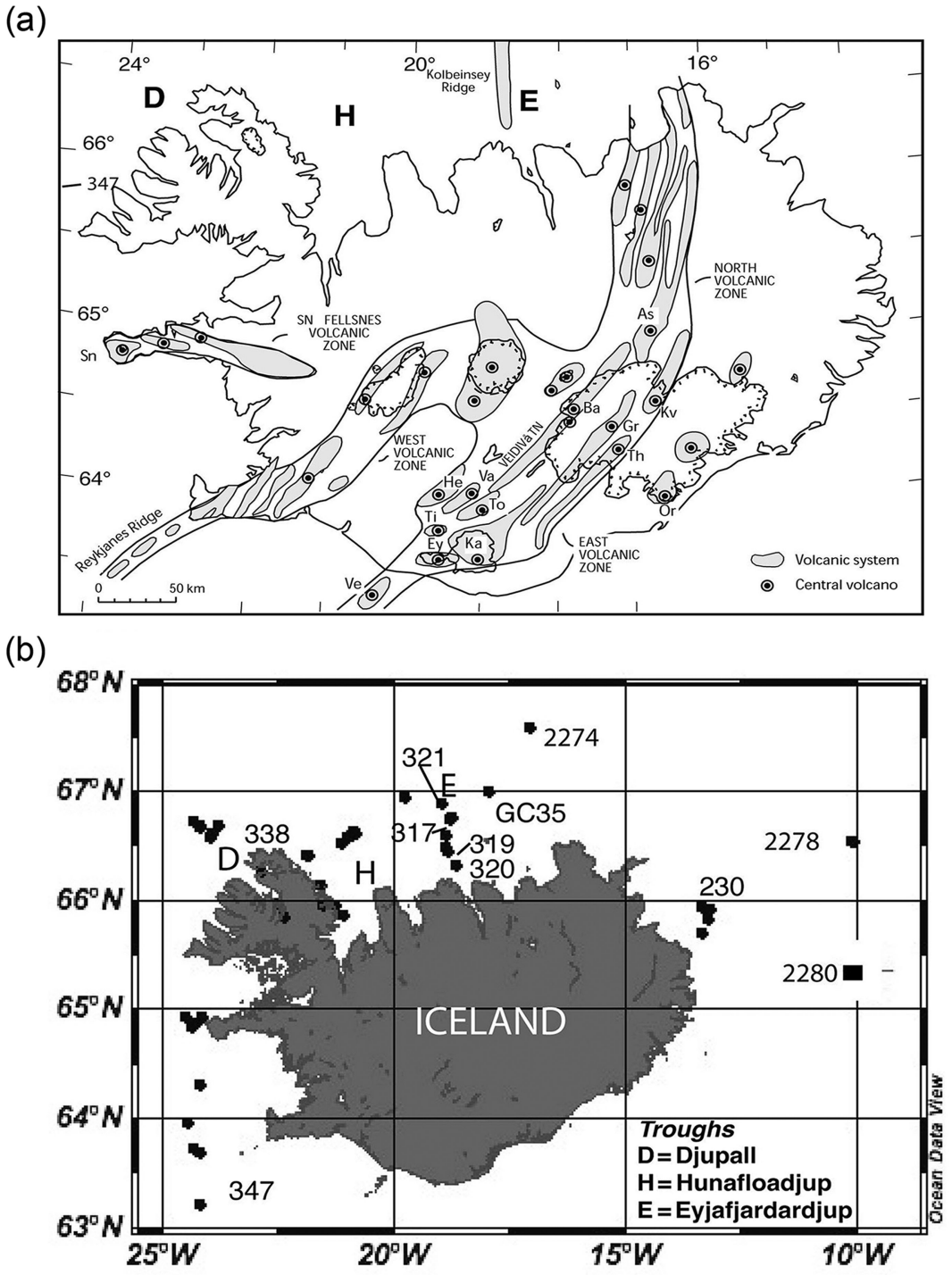

Fig. 1 (a) Map of the major volcanic zones of Iceland (based on Johannesson & Saemundsson 1998). D, H and E refer to major trough names. (b) Location of surface and/or down-core sediment sample sites around Iceland. See Supplementary Table S1 for details.

basaltic and rhyolitic eruptions (i.e., number of events per 1000 yr).

There is a fundamental difference between a tephra inventory based on soils, peats and lake sediments and those same eruptions recorded in marine sediment archives. In the former cases the tephra are often preserved as discrete sedimentary units (Thompson et al. 1986), whereas in the marine realm, slower rates

Citation: *Polar Research* 2013, *32*, 11130, http://dx.doi.org/10.3402/polar.v32i0.11130

of sediment accumulation and active bioturbation mean that tephra events are usually not visible. We used the term cryptotephras for these "hidden" tephra events in an earlier paper (Andrews et al. 2006) and retain the usage here, although we note that it has also been used for situations where tephra shards are very sparse. Some tephras are also not visible just because they look the same as the background material, and you cannot tell the differences visually between reworked and primary tephra. As noted by Larsen & Eirkiksson (2008: 114):

> The allogenic sand component of marine sediments close to a volcanic source like Iceland is inevitably of volcaniclastic nature. Consequently, the background content of volcanic grains is rather high and the definition of a primary tephra deposit and the differentiation of primary versus secondary tephra are not straightforward.

However, the Saksunarvatn tephra (10.2 calibrated thousand years [cal Ky] B.P.; Haflidason et al. 2000; Andrews, Geirsdóttir et al. 2002) and the 11.98 cal Ky B.P. Vedde ash are both visible in most marine cores around Iceland that extend back to $>12\,000$ cal yr B.P.

In Icelandic marine sediments, tephras are commonly recognized by sieving and counting the number and type of tephra shards in the sand fraction (Eiríksson, Knudsen, Haflidason & Heinemeier 2000; Larsen et al. 2002; Kristjánsdóttir et al. 2007)—a very time-consuming process. As part of the VAST programme we have investigated alternative methods for tephra detection, including x-ray florescence (XRF; Balascio et al. in press) and image analysis (D'Anjou et al. unpubl. ms.). Although these methods are certainly applicable in situations where deposition from volcanic events represents distinct changes in mineralogy, their suitability in an area, such as the Iceland shelf, is unclear because of the high background of volcaniclastics and the consequently high magnetic susceptibility (Andrews & Hardardottir 2009). Recognition of tephras in marine or lake sediments has been accomplished by measuring magnetic susceptibility (Thompson et al. 1980; Rasmussen et al. 2003). However, there is no clear correlations between mass magnetic susceptibility peaks and tephra events in the North Iceland shelf core MD99-2269 (Kristjánsdóttir 2005), nor any of the B997 cores discussed below. Indeed, it is noteworthy that the basaltic Saksunarvatn tephra is a pronounced low in magnetic susceptibility (Andrews, Geirsdóttir et al. 2002).

One alternative exploratory method for finding tephras in marine sediments is described in this paper, based on quantitative x-ray diffraction (qXRD) analysis of the <2 mm sediment fraction. About 99% of the Holocene off-shore marine sediments around Iceland are in the <2 mm sediment fraction (Andrews, Kihl et al. 2002). In our case, the study of the mineralogy of marine sediments was primarily concerned with the identification of the history of drift ice (Moros et al. 2006; Andrews et al. 2009), and the possible identification of tephra events was a secondary outcome. In addition to being relatively rapid, the qXRD method provides the advantage of detecting tephras with a grain-size signature of <63 μm (common in the minor volcanic explosions in Iceland and in the distal tephras of north-west Europe [Dugmore et al. 1995; Pilcher et al. 2005]). The more traditional sieving and shard counting method, does not capture the <63 μm grain size. However, a combination of sieving and density separations is proving useful for cryptotephras identification in the 25–80 μm size range (Abbott et al. 2011).

It is critical to note that we differentiate between volcanic glass and tephra. Volcanic glass refers to the characteristic qXRD signal created primarily by amorphous silica (Fig. 2a), whereas tephra in the qXRD sense consists of the amorphous glass component plus the constituent minerals of the respective tephras (Fig. 2b; Supplementary Table S1). The glass component of tephra is obtained by trimming the constituent minerals, such as plagioclase, from the XRD pattern (compare Fig. 2a, 2b) using the PeakChopper software programme (Eberl 2003).

We set ourselves three main goals: (1) to estimate the fraction of the offshore Iceland Holocene sediment (<2 mm) that is volcaniclastic; (2) to compare the occurrence of peaks in qXRD-determined volcanic glass content to peaks of primary tephra shards in the ≥ 150 μm fraction; and (3) to develop an initial inventory of the number of Holocene tephra events that are recorded in the Icelandic marine archives.

In Supplementary File 1 and Supplementary Table S2, we evaluate how well quantitative XRD distinguishes between different (in silica content) volcanic glasses and other amorphous silica materials, such as diatoms, chert and ground quartz.

Methodology and data

This paper uses quantitative XRD methodology (Eberl 2003). By their very nature, amorphous materials, such as biogenic silica and volcanic glass, cannot be resolved with great accuracy and precision by qXRD as, in contrast to minerals such as quartz, calcite, or kaolinite, amorphous materials do not have a series of well-resolved XRD peaks (Fig. 2a, 2b). The time taken to process 100 sediment samples by qXRD includes 16 hr of sample

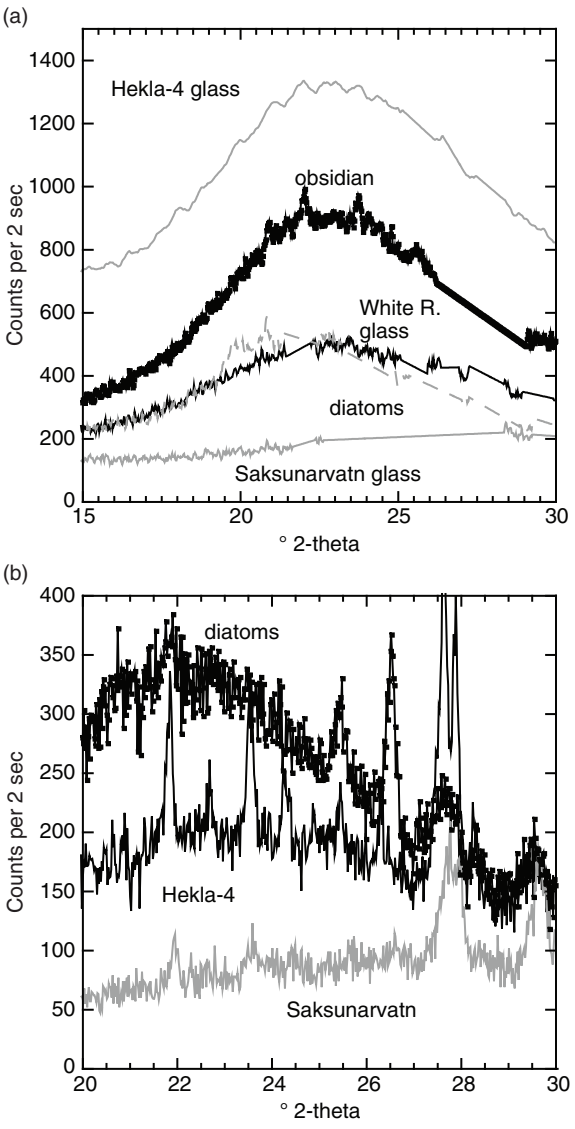

Fig. 2 (a) X-ray diffraction standard patterns from RockJock v6 showing the characteristic hump in amorphous materials between 15° and 30° 2-theta. Shown are the patterns for Hekla-4 volcanic glass, obsidian, White River volcanic glass, diatoms and Saksunarvatn volcanic glass. These plots have individual mineral peaks eliminated with the Peak-Chopper software program (Eberl 2003). (b) X-ray diffraction patterns for samples of Hekla-4 tephra (dark grey), Saksunarvatn tephra (light grey) and diatoms (black) prepared with the addition of ZnO (10% by wt). Note that for this plot the individual mineral peaks have not been eliminated by using PeakChopper. The difference in counts (y axis) compared to Fig. 2a is associated with the different preparation of standards vs. samples (Eberl 2003).

processing, 168 hr (7 days) of machine time, and 50 hr for data reduction. Most of the process is automated. This specific approach to quantitative XRD methodology has been successful in placing third twice and second place once in the international Reynolds Cup competitions using primarily qXRD (Omotoso et al. 2006). In this competition, "unknown" mineral mixes are sent to laboratories, which then have to provide their best estimates of the compositions (McCarty 2002; Omotoso et al. 2006). Briefly, 1 g of dry sediment is mixed with 0.111 g of zincite, ground for 5 min in a McCrone mill with the addition of 4 ml of ethyl alcohol. The McCrone mill reduces the grain size of the <2 mm sediment to <20 μm. The samples are dried in an oven at 80°C, sieved and loaded against frosted glass. The samples are then placed in a carousel and run on a Diffraktometer D5000 (Siemens, Munich, Germany) XRD unit from 5° to 65° 2-theta with a 0.02° 2-theta step, with a counting time of 2 sec per step, resulting in 3000 intensity measurements. The intensity data are then pasted into RockJock software (Eberl 2003), a Microsoft Excel Macro programme, and the patterns quantitatively compared with non-clay and clay mineral standards. RockJock determines the weight percent (wt%) of each species and calculates a degree-of-fit (DOF) statistic that is 0 for a perfect fit. The calculated total wt% should equal 100, but in practice usually varies between 95 and 110 wt%. The data are then normalized to sum to 100%.

RockJock v5 included White River tephra and glass (a rhyodacite tephra from Alaska [Robinson 2001]), diatoms (a Miocene diatomite from Oregon), obsidian, chert and a variety of opals. Subsequently in RockJock v6, Saksunarvatn and Hekla-4 tephra and glass were added as mineral standards (Fig. 2a shows the glass patterns). A new preparation method, using corundum, is now used in RockJock v11 (see Fig. 3) and also includes the three tephra and the three glass standards; we use version 6 to be consistent with earlier analyses (Andrews et al. 2006).

Initial tephra experiments

Initial experiments, using RockJock v5 (Andrews et al. 2006), added a known wt% of tephra to sediments and calculated the glass wt% from qXRD and showed good correlations ($r^2 > 0.8$). Furthermore, qXRD analyses of two cores off north Iceland were used to identify volcanic glass peaks based on the qXRD-determined wt% peaks; these in turn were verified by comparison with earlier counts of sand-size tephra shards. We also showed (Andrews et al. 2006) that there were differences in the qXRD patterns of basaltic vs. rhyolitic tephra, especially with regard to the 2-theta position of the maximum of the amorphous hump (e.g., Fig. 2a). The basaltic Saksunarvatn tephra, with an average silica content of ca. 45% (Andrews, Geirsdóttir et al. 2002), has a distinctly

Citation: *Polar Research* 2013, *32*, 11130, http://dx.doi.org/10.3402/polar.v32i0.11130

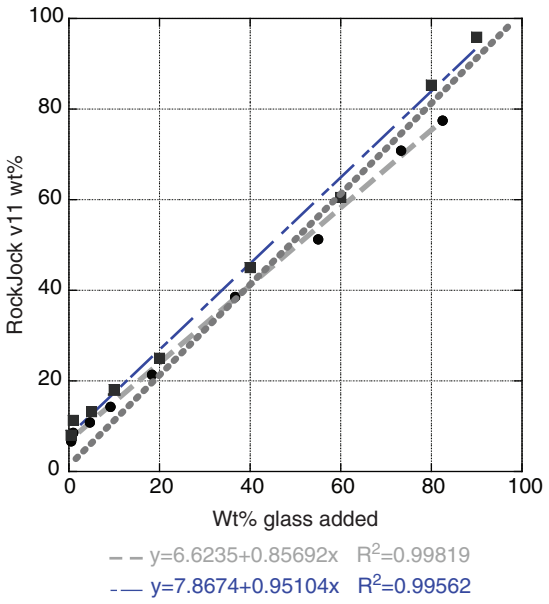

Fig. 3 Comparison of measured and calculated (RockJock v11) wt% of White River glass and tephra (x axis) to a ground-up granite. The dotted line shows the ideal curve that passes through the origin.

different pattern from the more silica-rich (ca. 65%) dacitic Hekla-4 tephra (Fig. 2). The wide range in composition of total alkali-silica in tephras (Le Maitre 1984) suggests that the accuracy of current qXRD estimates of glass wt% will not be very precise but still a useful approximation. Other amorphous materials result in somewhat similar broad humps in the diffraction pattern (i.e., diatoms and obsidian), although the opals (not shown) are distinctly different. Grinding of samples can also produce amorphous materials (O'Connor & Chang 1986; see Supplementary Table S2); in our tests some 25% of the sediment is <0.5 μm after 5 min of grinding.

Data used

The database for this study consists of qXRD analysis of discrete seafloor sediments ($n=49$) collected between 10° and 25°W and 63° and 68°N around Iceland, approximately 1200 discrete down-core samples, and the analysis of sediment cores from Iceland waters west of 18° longitude (B997-317, -319, -321 and -338) (Fig. 1b; Supplementary Table S1). The numbers of surface seafloor samples have been increased from that reported earlier (Andrews & Eberl 2007) by the addition of samples from the MD99-Leg 3 cruise, four samples from east Iceland supplied by the Iceland Marine Research Institute (G. Helgadóttir, pers. comm.) from Cruise AO390, sites nos. 230, 231, 235, 236 (Fig. 1b), and core JR51-GC35 at nearly 67°N and 18°W (Bendle & Rosell-Mele 2007).

Supplementary File 1 and Supplementary Table S2 show a series of analyses using RockJock v6 to ascertain how well we can distinguish between six known samples that all have high fractions of amorphous material. We prepared samples from Hekla-4 (a rhyolitic tephra), the basaltic Saksunarvatn tephra (donated by Dr A. Geirsdottir; see Jóhannsdóttir 2007), and a sample of nearly pure diatoms from core MD99-2317, East Greenland (Jennings et al. 2006). Additionally, in order to compare the composition of Icelandic basalts and the offshore marine sediments, we pulverized and ground ice-rafted basalt pebbles from north-west Iceland (Supplementary Table S2). The results from the ice-rafted pebbles indicated very low wt% of tephra or glass ($\leq 1.5\%$) in this bedrock.

New methodology and revision of RockJock to v11

Advances have been made in the preparation of samples for qXRD and are incorporated into the recent revision of RockJock v11, which can be downloaded at ftp://brrcrftp.cr.usgs.gov/pub/ddeberl/. Carefully weighed samples containing an internal standard (corundum) are ground in a McCrone mill with ethanol, dried, shaken with a high vapour pressure organic liquid (vertrel), sieved and then side-loaded into a sample holder to make a randomly oriented preparation. To test the accuracy and precision of this new qXRD method, we prepared samples of granite and a carbonate crust from Baffin Island and added 0.5%, 1% and 5% (and so on) weight of White River tephra (Fig. 3). The results are more accurate than the older method, which uses ZnO as the calibration spike and had r^2 values of 0.92–0.97 (Andrews et al. 2006). With the new method, the agreement between the measured and predicted has an r^2 value of 0.99 (Fig. 3). However, the intercepts are not zero and these experiments indicate that the lower limit for reliable detection is in the range of ≥ 10 wt%. The fact that we do not obtain a zero intercept indicates that the grinding process produces amorphous materials, which limits the detection of small additions of tephra (see Supplementary Table S2). Therefore, the qXRD method probably will not be applicable for distal sites in mainland and north-west Europe (van den Bogaard & Schmincke 2002). The development of the improved method for sample preparation and enhancements in RockJock v11 (e.g., Omotoso et al. 2006) should also improve the overall ability of qXRD to detect increases in glass content associated with tephra deposition (Fig. 3), although paired tests of samples using zincite (RockJock

v6) vs. corundum (RockJock v11) failed to reveal consistent reduction in the precision of estimates of the wt% of known mineral mixtures.

Effect of using different volcanic glass standards

In our earlier work (Andrews et al. 2006), only the White River glass standard (RockJock v5) was used to derive the volcaniclastic wt% estimates. As can be seen in Figure 2a, White River glass is intermediate in both its qXRD pattern and in silica content between the Hekla-4 glass and Saksunarvatn glass standards. All the samples were initially evaluated using only the White River glass standard (RockJock v5). Subsequently, the data were re-run to evaluate whether we could distinguish between these two Icelandic "compositional end-members" of the tephra spectrum (RJ version 6). Diatoms were also added to the potential mineral mix because of the overlap between their XRD pattern and that of Hekla-4 glass (Fig. 2; Supplementary Table S2). However, in most instances, the wt% that can be ascribed to diatoms was a small wt% fraction.

Sediment samples from core B997-321PC subjected to qXRD analysis (Andrews et al. 2006) showed that the association between the original White River glass wt% (using RockJock v5) and the combined Saksunarvatn G and Hekla-4G wt% (using RockJock v6) is statistically highly significant, $r^2 = 0.83$ (Fig. 4a). As these are independent measures, the appropriate regression method is the reduced major axis (Till 1974). Estimates of the slope are similar in both methods, with 1.01 for reduced major axis vs. 0.92 for ordinary least squares. Examination of other cores where the White River glass wt% and Saksunarvatn glass + Hekla-4 glass wt% were compared, also resulted in the White River glass underestimating the glass wt% by 17–22 wt%. Thus, the application of only the White River glass standard underestimates the volcaniclastic fraction in the Iceland offshore sediment pile (Andrews 2007), but, importantly, it faithfully tracks the relative temporal variations in glass input.

Data from core B997-321PC (321 in Fig. 1b) indicated that the correlations between sand-sized (>150 μm) counts of fresh tephra grains, and the qXRD wt% of the <2 mm sediment is $r^2 = 0.29$ for the total fresh shard count (light [rhyolitic] + dark [basaltic]) and total glass wt% (Fig. 4b), $r^2 = 0.24$ for fresh, light shards vs. Hekla-4G and essential 0.0 for fresh dark grains vs. Saksunarvatn G (last two graphs not shown). These poor correlations reflect the fundamental differences in estimates based on bulk sediment vs. a restricted sediment fraction (e.g., sand).

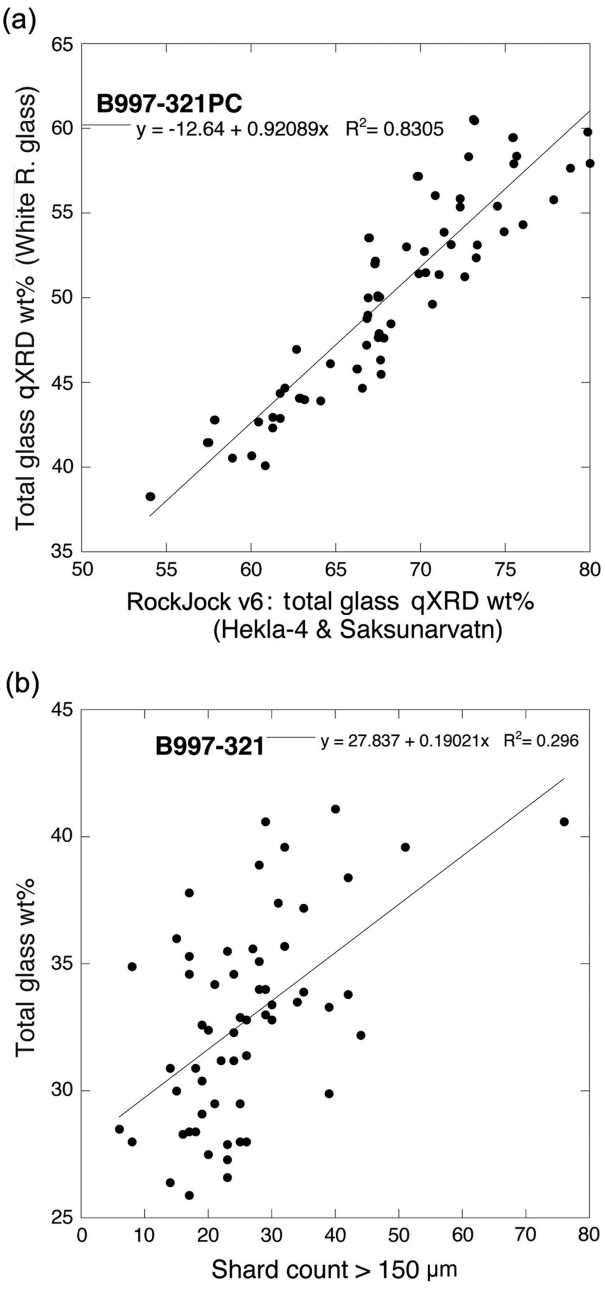

Fig. 4 (a) Scatter plot of total glass x-ray diffraction (qXRD) wt% using the White River glass standard and RockJock v5 (see Fig. 6 in Andrews et al. 2006) vs. the combined wt% of Hekla-4 glass and Saksunarvatn glass from B997-321PC using RockJock v6. (b) Comparison of the total counts of tephra shards >150 μm in B997-321PC with wt% estimates of total glass from qXRD analyses (RockJock v6).

Application of qXRD to Icelandic shelf sediments

We evaluate the results of our data generation under the three goals noted earlier. All the data are based on the standards in RockJock v6. In order to derive estimates

Citation: *Polar Research* 2013, *32*, 11130, http://dx.doi.org/10.3402/polar.v32i0.11130

of the spatial and temporal variations of the input of tephra and volcanic glass over 1200 samples from surface samples and cores around the Iceland margin are examined by qXRD. Note that: (1) there is little difference between wt% estimates of tephra and volcanic glass (see Fig. 3); and (2) pulverized basalt (Supplementary Table S2) contains little wt% glass. Therefore, for the purpose of this paper we equate volcaniclastic sediment with the wt% of glass. Such sediments are contributed to the Icelandic shelf through a variety of processes, including reworking of primary tephras by bottom processes, transport of volcaniclastic sediments in sediment meltwater plumes and wind transport (Prospero et al. 2012).

Estimation of the fraction of volcaniclastic sediments

Forty-nine sediment samples were run through qXRD analysis. Glass wt% is the sum of all three volcanic glass types. Relatively low glass wt% occurs in samples from the fjords and inner shelf (e.g., B997-332) and from B997-320 in Eyjafjardarall (Figs. 1b, 5a). This reflects some combination of dilution of sediments derived from local bedrock

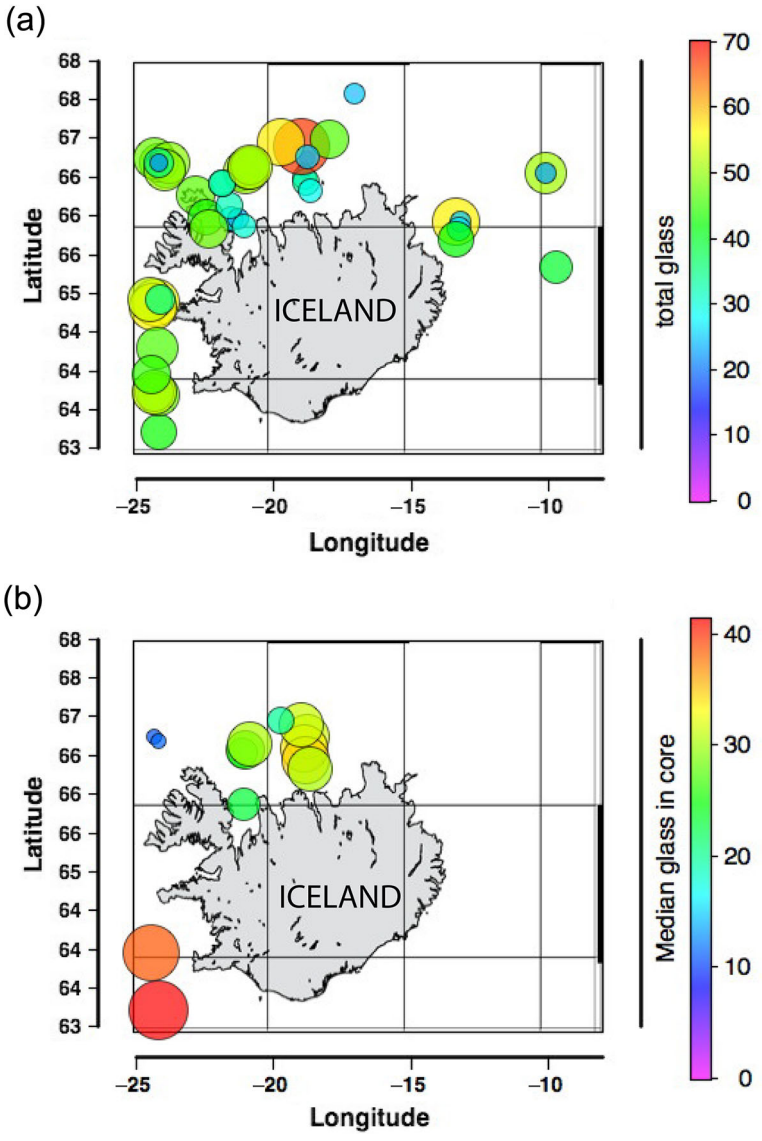

Fig. 5 (a) Wt% of total volcanic glass in surface samples. (b) Median wt% of volcanic glass in the cores (Table 1). Note that in these plots some of the individual sites are not visible because of the spatial overlap.

erosion, the abundance of biogenic carbonate and the overall location of the Icelandic volcanic system (Fig. 1a), with respect to the prevailing winds. We have no cores from the southern area of Iceland, which is dominated by massive glacial outburst floods (Maria et al. 2000).

Longer-term trends in the distribution of volcaniclastic sediments on the Iceland shelf can be seen in the distribution of median wt% glass in each of the cores (Supplementary Table S1; Fig. 5b). This pattern shows reduced glass content in north-west Iceland (<20 wt%), a moderate influx into Hunafloadjup, and higher wt% median values of glass along Eyjafjardarall (we have no cores east of 18°W longitude). High values of ca. 40 wt% (two cores) also occur in sediments from the south-west shelf (Fig. 5b).

These results support the assertion by Larsen & Eiríksson (2008) of the importance of volcaniclastic sediments in the Holocene archives of Iceland.

Comparison of down-core tephra counts and qXRD results

Figure 5 indicates that the sediments on the Iceland shelf have a significant fraction of volcaniclastics. As noted earlier, the "definition of a primary tephra deposit and the differentiation of primary vs. secondary tephra are not straightforward" (Larsen & Eiríksson 2008: 114).

In order to detect potential primary tephras, we follow the protocol discussed in Andrews et al. (2006); that is, positive residuals (>90% probability) from a fourth-order polynomial trend of glass wt% vs. depth were plotted for fresh light and dark tephra shard counts, and for glass wt%. Although qXRD samples were obtained from the same sediment splits as the tephra counts, we do not expect a one-to-one correspondence between shard counts and XRD-derived glass peaks for the following reasons: (a) there is a difference in grain size (>150 μm vs. <2 mm); (b) only fresh looking shards were counted as tephra; and (c) there is inherent sample variability.

Examples of the association between counts of tephra in the >150 μm size fraction and qXRD glass wt% were presented from core B997-321PC (Fig. 1b; Andrews et al. 2006); here we expand that examination to include additional data from cores B997-317PC1 and -319PC2 (Fig. 1b; Supplementary Table S1). These cores (Kristjánsdóttir 1999) have counts of fresh dark (basaltic) and fresh light (rhyolitic) tephra grains in the >150 μm fraction, which we compare to qXRD glass wt%. Reworked tephra grains were also counted but categorized as "other lithic grains". Accelerator mass spectrometry (AMS) ^{14}C dates are available for these cores as well as geochemistry on discrete shards from some of identified tephra peaks (Table 1) using the Nordic Volcanological Institute's microprobe (Grönvold et al. 1995; Supplementary Table S3).

The goal in this section is to see how well the qXRD estimates of glass wt% match tephra counts, and thus confirm or repudiate the qXRD approach as an exploratory tool. Clearly, additional geochemical analyses would be appropriate for fingerprinting specific tephras, but the number of analyses and the age control are sufficient to suggest possible candidates. Figures 6–8 plot the data vs. depth and include all available calibrated AMS ^{14}C dates (using the Calib 5 software program available at http://calib.qub.ac.uk/calib/calib.html) and a ΔR of 0 (Stuiver et al. 1998); age estimates are based on interpolation. Details of the radiocarbon dates are given in two date lists from the Institute of Arctic and Alpine Research, University of Colorado (Smith & Licht 2000; Quillmann et al. 2009). A ΔR of 0 appears appropriate for the time of the Saksunarvatn tephra (Andrews, Geirsdóttir et al. 2002), but in the late Holocene positive departures from a ΔR of 0 are evident around Iceland (Kristjánsdóttir 2005; Ascough et al. 2009; Eiríksson et al. 2010) and across the North Atlantic (Sjerup et al. 2010).

Core B997-317PC1. This core extends back to 3500 cal yr B.P. at 160 cm with four light and five dark tephra residual peaks. The dark (basaltic) peak at 20 cm in B997-317PC1 (Fig. 6, Table 1) is matched by a residual glass peak, which is dated to ca. 1600 AD based on interpolation between the two bounding dates (Fig. 6b). Tephra counts show a large peak in rhyolitic tephra at ca. 55 cm, which is matched by a large positive residual in glass content (Fig. 6c). This peak has the geochemical signature of Hekla-1104. Down-core, the peak in light tephra at 135 cm matches the age and composition for Hekla-3, although the residual glass content is only slightly positive. The rhyolitic peak at 162 cm occurs below an unconformity with a date of about 11 cal Ky B.P. The residuals from the lithic counts (Fig. 6d), which are dominated by reworked tephra grains, show some association with the glass residuals, such as the peak at 90 cm, but the statistical association is not significant.

Core B997-319PC2. This core extends back to ca. 7 Ky cal B.P. (Fig. 7c). The residual light tephra counts have three or four well-defined peaks, whereas the residuals from the dark tephra counts are much broader and define three main events. The residual glass peak at 60 cm (ca. 2500 cal yr B.P.) has no geochemistry data but matches to some extent with the dark tephra residuals. The large

Citation: *Polar Research* 2013, *32*, 11130, http://dx.doi.org/10.3402/polar.v32i0.11130

Table 1 Geochemical data for cores B997-317PC1, -3129PC2 and -338PC (see Kristjánsdóttir 1999 and Supplemental Table S3). Figures in parentheses after average is the number of analyses.

	SiO_2	TiO_2	Al_2O_3	FeO total	MnO	MgO	CaO	Na_2O	KO	P_2O_3	Total
B997-317PC1											
20–21.5 cm											
Average (8)	49.74	1.33	13.61	12.44	0.21	6. 99	10.91	2.39	0.09	0.13	97.8
SD	0.64	0.22	0.21	0.34	0.02	0.16	1.00	0.10	0.05	0.10	
55–56.25 cm											
Average (5)	71.16	0.20	14.19	3.16	0.10	0.11	1.95	4.21	2.68	0.02	97.8
SD	0.58	0.04	0.12	0.06	0.01	1.01	0.05	0.06	0.06	0.02	
135–136.25 cm											
Average (8)	71.67	0.30	13.34	3.81	0.16	0.21	1.34	4.95	3.24	0.16	99.2
SD	0.89	0.02	0.22	0.04	0.02	0.02	0.03	0.15	0.14	0.28	
Average (10)	71.70	0.30	13.56	3.81	0.14	0.21	1.31	5.20	3.18	0.09	99.5
SD	1.34	0.03	0.27	0.07	0.03	0.01	0.02	0.14	0.07	0.03	
Average (4)	49.25	4.20	12.70	14.00	0.22	4.59	9.09	3.25	0.85	0.85	99.0
162.5–163.75 cm											
Average (7)	49.62	1.49	14.55	11.13	0.21	7.48	12.45	2.26	0.15	0.18	99.5
SD	0.64	0.03	0.38	0.18	0.02	0.14	0.42	0.09	0.01	0.10	
Average (4)	48.67	4.51	12.08	13.98	0.22	4.83	9.16	NA	NA	NA	97.6
235–236.25 cm											
Average (2)	73.59	0.32	13.41	3.95	0.17	0.22	1.36		3.29	0.03	96.34
Average(4)	48.67	4.51	12.08	13.98	0.22	4.83	9.16	2.91	0.8	0.43	97.59
SD	0.99	0.25	0.28	0.61	0.02	0.27	0.49	0.12	0.13	0.03	
B997-319PC2											
105–106.75 cm											
Average (5)	71.73	0.21	14.15	3.19	0.09	0.10	1.95	3.99	2.75	0.01	98.2
SD	0.90	0.05	0.27	0.08	0.01	0.01	0.07	0.13	0.08	0.01	
	46.28	4.53	12.96	14.23	0.18	5.06	9.08	3.13	0.71	0.51	96.7
	46.92	4.50	13.04	14.57	0.19	5.07	9.50	3.09	0.72	0.95	98.6
150–151.25 cm											
Average (3)	70.28	0.29	14.46	4.05	0.14	0.19	2.56	3.91	2.47	0.02	98.4
208.75–210 cm											
Average (5)	50.06	3.03	12.45	13.82	0.24	5.41	9.49	2.76	0.44	0.34	98.0
SD	0.32	0.06	0.22	0.16	0.02	0.12	0.22	0.05	0.03	0.03	
	73.28	0.31	11.54	3.83	0.14	0.20	1.26	1.93	1.46	0.03	95.6
218.75–220 cm											
Average (3)	72.89	0.34	13.81	3.96	0.17	0.20	1.38		3.33	0.05	96.1
B997-338PC											
90 cm	78.68	0.15	13.15	3.20	0.06	0.00	0.45	1.58	3.18	0.02	100.5
	78.30	0.15	13.28	3.33	0.08	0.00	0.44	1.72	3.14	0.04	100.5
	79.29	0.19	12.78	3.36	0.02	0.00	0.47	0.79	2.65	0.00	99.5
Average	78.80	0.20	13.10	3.30	0.10	0.00	0.50	1.40	3.00	0.00	100.2
SD	0.50	0.00	0.30	0.10	0.00	0.00	0.00	0.50	0.30	0.00	0.5
99–101 cm	75.82	0.41	10.53	7.65	0.16	0.00	0.43	1.47	2.91	0.01	99.4
	75.76	0.44	10.33	7.57	0.18	0.01	0.42	1.51	3.15	0.00	99.4
	75.83	0.42	10.60	7.68	0.22	0.00	0.42	1.13	2.42	0.01	98.7
	76.91	0.15	12.90	3.33	0.05	0.02	0.37	1.69	3.72	0.00	99.1
	80.01	0.15	13.10	3.13	0.08	0.01	0.39	0.25	2.15	0.00	99.3
	77.57	0.20	13.30	3.25	0.06	0.03	0.41	1.67	3.82	0.00	100.3
	76.19	0.38	10.61	7.92	0.22	0.02	0.37	1.55	3.34	0.02	100.6
	77.47	0.49	10.53	7.79	0.20	0.00	0.39	1.22	2.51	0.01	100.6
	78.64	0.10	13.25	3.26	0.08	0.01	0.36	1.79	3.48	0.00	101.0
Average	77.10	0.30	11.70	5.70	0.10	0.00	0.40	1.40	3.10	0.00	99.8
SD	1.50	0.20	1.40	2.40	0.10	0.00	0.00	0.50	0.60	0.00	0.8

Table 1 *Continued*

	SiO_2	TiO_2	Al_2O_3	FeO total	MnO	MgO	CaO	Na_2O	KO	P_2O_3	Total
190 cm	77.53	0.18	13.09	3.20	0.09	0.00	0.37	1.79	3.35	0.00	99.6
	76.95	0.19	13.17	3.29	0.08	0.00	0.40	1.82	3.36	0.01	99.3
	77.03	0.18	13.06	3.19	0.07	0.01	0.37	1.88	3.59	0.03	99.4
	66.68	0.52	16.78	4.18	0.12	0.41	1.49	4.57	4.72	0.06	99.5
	65.22	0.38	17.91	4.12	0.05	0.32	2.20	5.20	3.90	0.08	99.4
	72.81	0.21	13.04	4.68	0.09	0.09	2.02	1.65	2.15	0.01	96.8
	74.78	0.20	13.35	4.84	0.07	0.07	2.13	1.45	2.29	0.03	99.2
	76.95	0.20	12.86	3.31	0.07	0.01	0.35	1.79	4.08	0.00	99.6
	77.80	0.21	12.78	3.23	0.09	0.01	0.37	1.67	3.47	0.01	99.6
Average	74.00	0.30	14.00	3.80	0.10	0.10	1.10	2.40	3.40	0.00	99.2
SD	4.80	0.10	1.90	0.70	0.00	0.20	0.90	1.40	0.80	0.00	0.9
192–194 cm	77.96	0.14	12.92	3.30	0.04	0.00	0.42	1.68	2.88	0.00	99.3
	77.72	0.18	13.26	3.21	0.06	0.00	0.38	1.65	2.80	0.02	99.3
	77.68	0.16	13.02	3.28	0.05	0.00	0.40	1.63	3.15	0.00	99.4
	77.32	0.16	13.21	3.22	0.05	0.00	0.41	1.78	3.17	0.00	99.3
	77.70	0.14	13.18	3.15	0.06	0.00	0.43	1.57	3.00	0.00	99.2
	77.19	0.19	13.34	3.18	0.07	0.02	0.42	1.72	3.07	0.00	99.2
	77.85	0.20	13.01	3.33	0.04	0.00	0.44	1.70	2.99	0.02	99.6
	78.31	0.16	13.03	3.17	0.03	0.00	0.42	1.56	2.80	0.00	99.5
	78.09	0.20	13.12	3.11	0.03	0.00	0.39	1.69	2.90	0.01	99.6
Average	77.10	0.30	11.70	5.70	0.10	0.00	0.40	1.40	3.10	0.00	99.8
SD	1.50	0.20	1.40	2.40	0.10	0.00	0.00	0.50	0.60	0.00	0.8

glass residuals at about 100 cm depth are matched by the light tephra residuals and have an interpolated age of ca. 3200 cal yr B.P. and a geochemistry that suggests a correlation with Hekla-3 (Table 1). A prominent light tephra and glass residual peak is bracketed by two radiocarbon dates, which together suggest a correlation with Hekla-Selsund/Kebister tephra (Wastegård et al. 2008). However, the geochemical signature of the tephra (Table 1) may not support such a correlation because the FeO and CaO values are too high. The substantial peak in light tephra at ca.180 cm (ca. 4500 cal yr B.P. by interpolation) is matched by a residual glass peak, but no geochemical analyses have been undertaken from this event; it is, however, a Hekla-4 candidate. The residuals from the lithic counts (Fig. 7d) show no particular association with the glass wt% residuals but they do mimic, to some degree, the residual dark tephra peaks (Fig. 7b, 7d). There is no peak in lithics (reworked tephra) at, for example, 100 cm, suggesting that the glass wt% may be responding to tephra in the <150 μm sediment.

Core B997-338PC. Data from this core are included here to show the exploratory potential of the qXRD method. Core B997-338 (338 in Fig. 1b) has a basal diamict unit (Dmm) and, based on initial radiocarbon dates, was considered to represent most of Marine Isotope Stage 2 (Andrews, Hardardóttir et al. 2002) with pulses of ice-rafted sedimentation (Fig. 8); additional radiocarbon dating revealed that this interpretation was incorrect (Olafsdóttir 2004; Chesley 2005). Careful examination of several samples revealed the presence of small, delicate articulated shells, which were AMS ^{14}C dated (Table 2, Fig. 8). There are several peaks in residual glass percentage in the core, and earlier, visual examination of the ≥ 120 μm fraction revealed the presence of fresh tephra shards at several levels, although detailed point-counts were not undertaken (Chesley 2005). The youngest event at ca.10 cm probably represents reworking of the widespread Vedde ash. Of particular interest here are the two positive residuals of total glass wt% from qXRD at ca. 100 and 200 cm (Fig. 8). These levels were investigated to reveal fresh tephra shards (Table 1). Based on the new radiocarbon dates, these tephras are amongst the oldest "postglacial" eruptions found in the area of Iceland (Haflidason et al. 2000; Andrews & Helgadottir 2003) as they potentially date from 15.5–14.7 cal Ky B.P. (assuming a 400 yr ocean reservoir correction, although the magnitude of the ocean reservoir correction for this period is uncertain). The basal diamicton unit also contains several residual glass peaks (Fig. 8).

Eiríksson and co-workers (Eiríksson, Knudsen, Haflidason & Henriksen 2000) and Andrews & Helgadóttir (2003) tentatively identified Borrobol tephra, originally found in Scotland (Turney et al. 1997; Davies et al. 2004),

Citation: *Polar Research* 2013, *32*, 11130, http://dx.doi.org/10.3402/polar.v32i0.11130

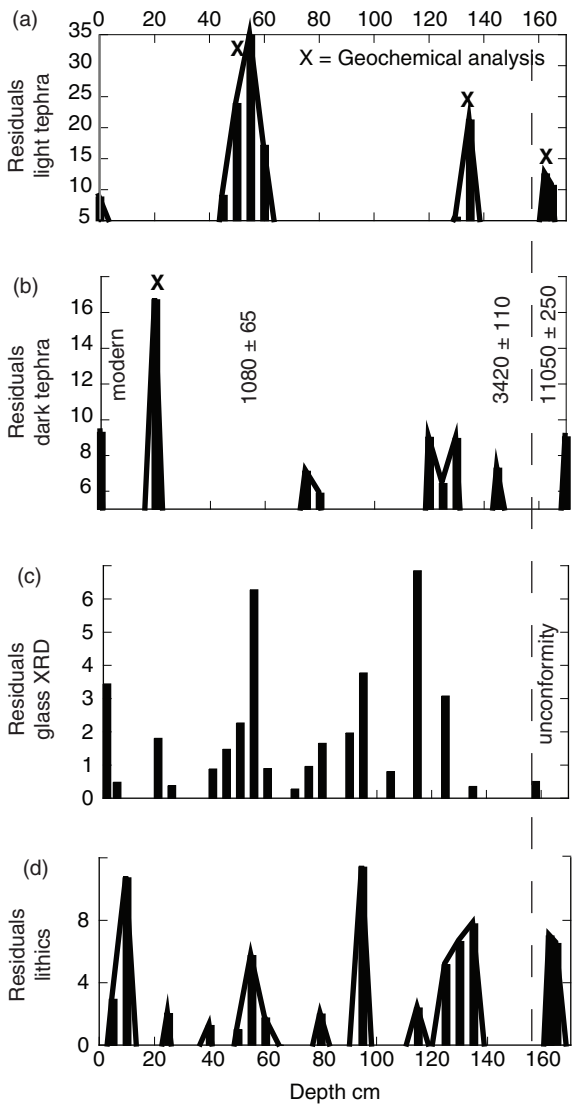

Fig. 6 Plots vs. depth of residuals from percentages of tephra shards >150 μm in core B997-317PC1: (a) fresh light (rhyolitic) and (b) fresh dark (basaltic; see Fig. 1b) vs. residuals (c) from the wt% total glass content from the <2 mm sediment; and (d) residuals from lithic counts (which include reworked tephra). Calibrated radiocarbon dates are shown including one ''modern''. The line at ca.160 cm represents an apparent unconformity as the tephra at 162 cm has a Vedde-like composition and calibrated date of 11 050 ± 250 Ky B.P. X represents levels where geochemical analyses have been undertaken (see Table 2) on individual handpicked tephra shards.

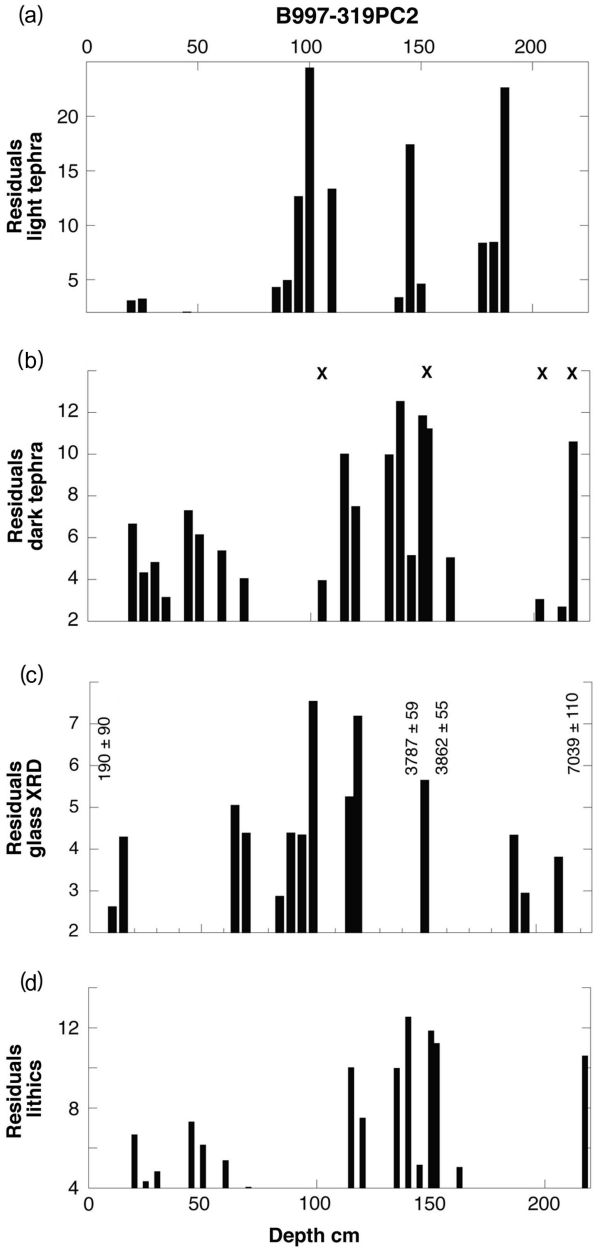

Fig. 7 Plots vs. depth of residuals from percentages shards >150 μm in core B997-319PC2 (Fig. 1b) of (a) light and (b) dark tephra vs. residuals (c) from the wt% total glass content from the <2 mm sediment; and (d) residuals from lithic counts. Calibrated radiocarbon dates are shown (Table 2). X represents levels where geochemical analyses have been undertaken (see Table 2) on individual handpicked tephra shards.

in cores off northern Iceland. The best current age range for the Borrobol tephra is 13.95–14.14 cal Ky B.P. (Matthews et al. 2011). Therefore, if one of the tephras in B997-338 (Fig. 8) is coeval with the Borrobol tephra then the ocean reservoir correction would have to be of the order of 1000 ± yr, which cannot be ruled out, and is indeed likely (Thornalley et al. 2011). However, there are at least two distinct tephra events separated by ca. 100 cm of sediment (Fig. 8), and it is therefore tempting to hypothesize that this core might also contain the younger Penifiler tephra, also found in Scotland (Pyne-O'Donnell et al. 2008). The major element chemistry for the two tephras in B997-338 (Table 1; analysis at the University of

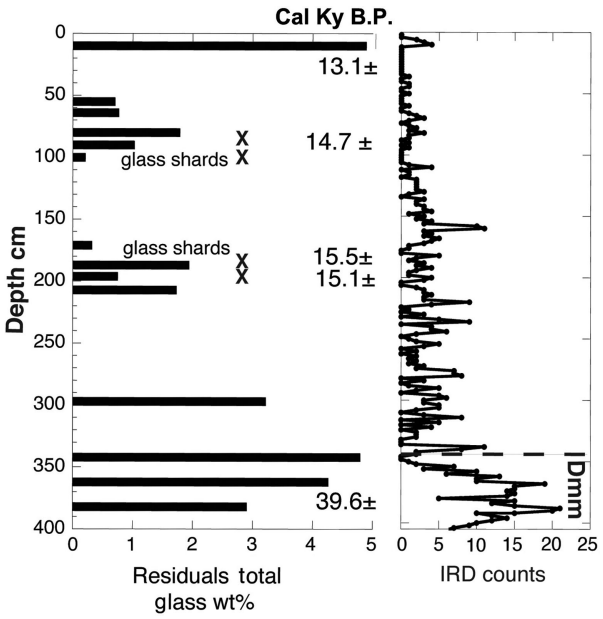

Fig. 8 Down-core plot of data from B997-338, off north-west Iceland (Fig. 1b) showing residual glass peaks, levels for geochemical analyses (X), calibrated radiocarbon dates ($\Delta R = 0$) and counts of ice-rafted debris (IRD) >2 mm/14 cm^2 from x-radiographs. X represents levels where geochemical analyses have been undertaken (see Table 2) on individual handpicked tephra shards.

Colorado Microprobe Laboratory; see Supplemental File 2) have some similarities with these named tephras (Matthews et al. 2011), but more chemistry is required to rigorously establish provenance. Potentially correlative silica-rich tephras have been noted in the North Greenland Ice Core Project core (Mortensen et al. 2005).

Holocene inventory of tephra events in marine cores by qXRD

Background volcaniclastic (ca. glass wt%) values are shown as the median wt% in the cores (Fig. 5b), but we raise the question of whether we can detect significant coherent tephra events in all these marine cores. Based on our initial exploratory investigation, and the results presented above, we expand the analysis to the total set of cores that we have run for qXRD (Andrews 2009). We employed the same protocol used earlier; that is, we fitted the down core data to a fourth-order polynomial and then only considered possible tephra events as being that wt% of glass that was >90% of the values for that particular core; we refer to these as "probable events". These data were then plotted against cal yr B.P. using the existing depth/age models for each core. The next step was to derive an estimate of the number of probable events per 1000 yr for each core and then combine them into an estimate of the number of tephra events in the size range <2 mm captured in the offshore marine archives (Fig. 9). Calculating events per 1000 yr reduces bias imposed by the fact that the number of 1000 yr intervals varies because of the age estimates for the core tops and basal sediments.

The results indicate that the number of tephra events preserved over the last 12 000 cal yr B.P. on the Iceland shelf has not been constant. Minima are recorded for the 3–5 and 8–10 cal Ky B.P. intervals, and peaks in events occur at 12 and 7 (minor) Ky B.P. and during the last 1 cal Ky B.P. The events graphed in Fig. 9 include both silica-rich and basaltic events and hence are not strictly comparable with the frequency graphs of Larsen & Eiríksson (2008, e.g., their figure 4), which are for tephras with silica values >63% and >54%. Both records show a major increase over the last 1 cal Ky B.P. and lower numbers between 4 and 10 cal Ky B.P. Our marine data (Fig. 9) do not pick up the major peak in events centred around 3 cal Ky B.P. This may be associated with the intensity of the eruptions and the plume trajectory.

Discussion and conclusions

One of the goals of VAST was to see whether we could develop rapid, exploratory methods for detecting tephras in lake and marine sediments. In the last one to two decades, tephra chronology has become an increasingly important chronological tool in the northern North Atlantic and north-west Europe (Dugmore et al. 1995;

Table 2 Comparison of the ''old'' dates (left column) on B997-338PC vs. the new dates on articulated bivalves. The calibrated ages assume a ΔR of zero; see text for discussion. Dates were calibrated in Calib 5 software program. Asterisks indicate suspect dates.

Depth (cm)	^{14}C date	Error	Cal yr B.P.	Error	Dated material
20.5	11560	170	13057	131	Benthic forams
98.5	13020	220	14731	383	New date on articulated bivalve
99.5*	19280*	420	22564	604	Benthic forams & bivalve
194	13507	78	15477	183	New date on articulated bivalve
210	13235	62	15134	125	New date on articulated bivalve
319.5*	31900*	1700	36883	1700	Benthic forams
412	34600	640	39568	645	Benthic forams

Citation: *Polar Research* 2013, *32*, 11130, http://dx.doi.org/10.3402/polar.v32i0.11130

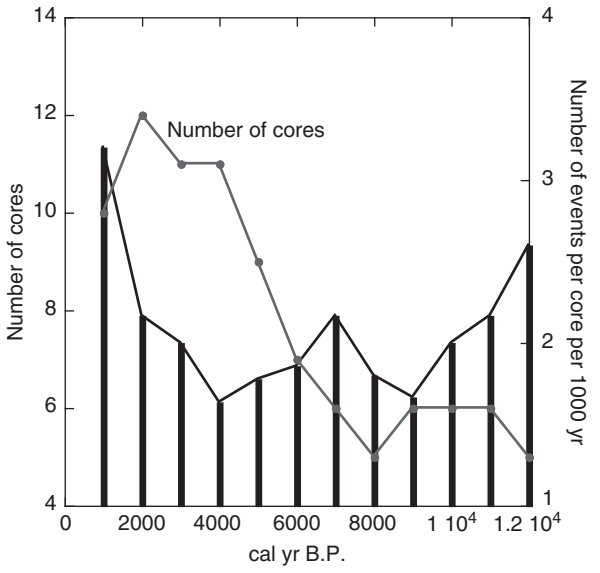

Fig. 9 Plots of number of probable tephra events per 1000 yr from counts of the residual glass wt% plots (e.g., Figs. 7, 8) and the number of cores for each 1000 yr interval (grey line with filled circles).

Haflidason et al. 2000; Larsen et al. 2002; Kristjánsdóttir et al. 2007; Wastegård & Davies 2009). In Icelandic marine sediments, tephras are usually not visible to the naked eye nor on x-radiographs; hence, their recognition frequently requires a time-consuming process of sieving and density separation. However, because of sorting during transportation and depositional processes (Lacasse 2001), not all tephra events are recorded as sand-size shards, especially in more distal locations.

The purpose of our investigations within the framework of VAST was to investigate whether there are exploratory approaches that would assist in narrowing the search for cryptotephras by using scanning XRF, image analysis or qXRD. Such experimental investigations (Kylander et al. 2012) are important when we are dealing with very high-resolution marine sediment archives involving tens of metres of sediment, such as the giant Calypso cores taken around Iceland and in the North Atlantic involving 10–50 m of Holocene sediment (Labeyrie et al. 2003). Our experimental approach of seeding minerogenic (ground bedrock) with known wt% of tephra (Fig. 3) indicates that the method has significant potential for the identification of tephras, and the recognition of samples that would then benefit from further detailed investigation. Because of the high volcaniclastic background of glass content in the Icelandic shelf sediments, our investigation of down-core variations in glass content using qXRD is undertaken in probably the worst conditions for detecting discrete tephras. However, we have shown that for four cores—B997-317, -319, -321 and -338 (Figs. 4, 6–8)—qXRD of the total sediment fraction <2 mm offers a reproducible and robust approach to the identification of tephra events within a core, including events whose grain size is <63 μm. The qXRD method does not perform geochemical fingerprinting but it can point toward the type of tephra: basaltic, rhyolitic, or a more intermediate silica content (Fig. 2).

Acknowledgements

The majority of the cores and grab samples cores were collected in 1997 and 1999 on cruises of *Bjarni Saemundsson* and *Marion Dufresne*. This work has been supported by a variety of grants from the US National Science Foundation, including grants ATM-9531397 and 052515, OCE-9809001 and OPP 0326776 and 0714074, and the Icelandic Centre for Research. GBK's research was supported by the Icelandic Centre for Research grants nos. 981870098 and 981870099 to Dr A. Geirsdottir and an Icelandic Centre for Research Student Grant, Fulbright student grant and American Association of University Women student grant. We greatly appreciate the comments of Dr H. Haflidason and R. Bradley on an initial draft. We also appreciate the comments and suggestions of two reviewers on the original submitted version of this manuscript, and a further two reviewers on the revised manuscript. On publication all the data in this paper will be submitted to the National Oceanic and Atmospheric Administration's palaeoclimate database (www.ncdc.noaa.gov/paleo/data.html).

References

Abbott P.M., Davies S.M., Austin W.E.N., Pearce N.J.G. & Hibbert F.D. 2011. Identification of cryptotephra horizons in a North East Atlantic marine record spanning Marine Isotope Stages 4 and 5a (~ 60,000–82,000 a b2k). *Quaternary International 246*, 177–189.

Andrews J.T. 2007. Holocene denudation of Iceland as determined from accumulation of sediments on the continental margin. *Boreas 36*, 240–252.

Andrews J.T. 2009. Seeking a Holocene drift ice proxy: non-clay mineral variations from the SW to N-central Iceland shelf: trends, regime shifts, and periodicities. *Journal of Quaternary Science 24*, 664–676.

Andrews J.T., Darby D.A., Eberl D.D., Jennings A.E., Moros M. & Ogilvie A. 2009. A robust multi-site Holocene history of drift ice off northern Iceland: implications for North Atlantic climate. *The Holocene 19*, 71–78.

Andrews J.T. & Eberl D.D. 2007. Quantitative mineralogy of surface sediments on the Iceland shelf, and application to down-core studies of Holocene ice-rafted sediments. *Journal of Sedimentary Research 77*, 469–479.

Andrews J.T., Eberl D.D. & Kristjansdottir G.B. 2006. An exploratory method to detect tephras from quantitative XRD scans: examples from Iceland and East Greenland marine sediments. *The Holocene 16*, 1035–1042.

Andrews J.T., Geirsdóttir A., Hardardóttir J., Principato S., Grönvold K., Kristjansdóttir G.B., Helgadóttir G., Drexler J. & Sveinbjörnsdóttir A. 2002. Distribution, sediment magnetism, and geochemistry of the Saksunarvatn (10180 60± cal. yr BP) tephra in marine, lake, and terrestrial sediments, NW Iceland. *Journal of Quaternary Science 17*, 731–745.

Andrews J.T. & Hardardóttir J. 2009. A comparison of Holocene sediment- and paleo-magnetic characteristics from the margins of Iceland and East Greenland. *Jökull 59*, 51–66.

Andrews J.T., Hardardóttir J., Geirsdóttir Á. & Helgadóttir G. 2002. Late Quaternary ice extent and glacial history from the Djúpáll trough, off the Vestfirdir peninsula, north-west Iceland: a stacked 36 cal environmental record. *Polar Research 21*, 211–226.

Andrews J.T. & Helgadóttir G. 2003. Late Quaternary ice cap extent and deglaciation of Hunafloaall, northwest Iceland: evidence from marine cores. *Arctic, Antarctic, and Alpine Research 35*, 218–232.

Andrews J.T., Kihl R., Kristjánsdóttir G.B., Smith L.M., Helgadóttir G., Geirsdóttir Á. & Jennings A.E. 2002. Holocene sediment properties of the East Greenland and Iceland continental shelves bordering Denmark Strait (64°–68°N), North Atlantic. *Sedimentology 49*, 5–24.

Ascough P.L., Cook G.T. & Dugmore A.J. 2009. North Atlantic marine 14C reservoir effects: implications for late-Holocene chronological studies. *Quaternary Geochronology 4*, 171–180.

Balascio N., Francus P., Bradley R.S., Kvisvik B.C. & Thordarson T. in press. Investigating the use of scanning X-ray fluorescence to locatye cryptotephra in minerogenic lacustrine sediments: experimental results. *Journal of Limnology*.

Bendle J.A.P. & Rosell-Mele A. 2007. High-resolution alkenone sea surface temperature variability on the North Icelandic Shelf: implications for Nordic seas paleoclimatic development during the Holocene. *The Holocene 17*, 9–24.

Chesley T. 2005. *Mineralogy, sediment, and foraminiferal history of Djupall, Iceland: reconstructing a past record*. BA honours thesis, Dept. of Geological Sciences, University of Colorado, Boulder.

Davies S.M., Wohlfarth B., Wastegard S., Andersson M., Blockley S. & Possnert G. 2004. Were there two Borrobol Tephras during the early Lateglacial period: implications for tephrochronology? *Quaternary Science Reviews 23*, 581–589.

Dugmore A.J., Larsen G. & Newton A.J. 1995. Seven tephra isochrones in Scotland. *The Holocene 5*, 257–266.

Eberl D.D. 2003. *User's guide to RockJock—a program for determining quantitative mineralogy from x-ray diffraction data. Open File Report 03–78*. Washington, DC: United States Geological Survey.

Eiríksson J., Knudsen K.L., Haflidason H. & Heinemeier J. 2000. Chronology of late Holocene climatic events in the northern North Atlantic based on AMS ^{14}C dates and tehpra markers from the volcano Hekla, Iceland. *Journal of Quaternary Science 15*, 573–580.

Eiríksson J., Knudsen K.L., Haflidason H. & Henriksen P. 2000. Late-glacial and Holocene palaeoceanography of the North Iceland Shelf. *Journal of Quaternary Science 15*, 23–42.

Eiríksson J., Knudsen K.L., Larsen G., Olsen J., Heinemeier J., Bartels-Jónsdóttir H.B., Jiang H., Ran L.H. & Símonarson L.A. 2010. Coupling of palaeoceanographic shifts and changes in marine reservoir ages off north Iceland through the last millennium. *Palaeogeography Palaeoclimatology Palaeoecology 302*, 95–108.

Grönvold K., Oskarsson N., Johnsen S.J., Clausen H.B., Hammer C.U., Bond G. & Bard E. 1995. Ash layers from Iceland in the Greenland GRIP ice core correlated with oceanic and land sediments. *Earth and Planetary Science Letters 135*, 149–155.

Haflidason H., Eiríksson J. & Van Kreveld S. 2000. The tephrachronology of Iceland and the North Atlantic region during the Middle and Late Quaternary: a review. *Journal of Quaternary Science 15*, 3–22.

Jennings A.E., Hald M., Smith L.M. & Andrews J.T. 2006. Freshwater forcing from the Greenland Ice Sheet during the Younger Dryas: evidence from southeastern Greenland shelf cores. *Quaternary Science Reviews 25*, 282–298.

Jóhannsdóttir G.E. 2007. *Mid-Holocene to late glacial tephrochronology in west Iceland as revealed in three lacustrine environments*. MSc thesis, Institute of Earth Sciences, University of Iceland.

Kelly P.M. 1977. Volcanic dust veils and North Atlantic climatic change. *Nature 268*, 616–617.

Kristjánsdóttir G.B. 1999. *Late Quaternary climatic and environmental changes on the North Iceland shelf*. MSc thesis, Dept. of Geosciences, University of Iceland.

Kristjánsdóttir G.B. 2005. *Holocene climatic and environmental changes on the Iceland shelf: d18O, Mg/Ca, and tephrochronology of core MD99-2269*. PhD thesis, Dept. of Geological Sciences, University of Colorado, Boulder.

Kristjánsdóttir G.B., Stoner J.S., Grönvold K., Andrews J.T. & Jennings A.E. 2007. Geochemistry of Holocene cryptotephras from the North Iceland Shelf (MD99-2269): intercalibration with radiocarbon and paleomagnetic chronostratigraphies. *The Holocene 17*, 155–176.

Kylander M.E., Lind E.M., Wastegård S. & Lowemark L. 2012. Recommendations for using XRF core scanning as a tool in tephrochronology. *The Holocene 22*, 371–375.

Labeyrie L., Jansen E. & Cortijo E. 2003. *Les rapports de campagnes à la mer MD114/IMAGES V. (MD114/IMAGES V cruise report.)* Brest: Institut Polaire Francais Paul-Emile Victor.

Lacasse C. 2001. Influence of climatic variability on the atmospheric transport of Icelandic tephra in the subpolar North Atlantic. *Global and Planetary Change 29*, 31–56.

Larsen G. & Eiríksson J. 2008. Late Quaternary terrestrial tephrachronology of Iceland—frequency of explosive eruptions, type and volume of tephra deposits. *Journal of Quaternary Science 23*, 109–120.

Larsen G., Eiríksson J., Knudsen K.-L. & Heinemeir J. 2002. Correlation of late Holocene terrestrial and marine tephra markers, north Iceland: implications for reservoir age changes. *Polar Research 21*, 283–290.

Le Maitre R.W. 1984. A proposal by the IUGS subcommision on the systematics of igneous rocks for a chemical classification of volcanic rocks based on the total alkali silica (TAS) diagram. *Australian Journal of Earth Sciences 31*, 243–255.

Maria A., Carey S., Sigurdsson H., Kincaid C. & Helgadóttir G. 2000. Source and dispersal of jökulhaup sediments discharged to the sea following the 1996 Vatnajökull eruption. *Geological Society of America Bulletin 112*, 1507–1521.

Matthews I.P., Birks H.H., Bourne A.J., Brooks S.J., Lowe J.J., Macleod A. & Pyne-O'Donnell S.D.F. 2011. New age estimates and climatostratigraphic correlations for the Borrobol and Penifiler tephras: evidence from Abernethy Forest, Scotland. *Journal of Quaternary Science 26*, 247–252.

McCarty D.K. 2002. Quantitative mineral analysis of clay-bearing mixtures: the "Reynolds Cup" contest. *International Union of Crystallography Newsletter 27*, 12–16.

Moros M., Andrews J.T., Eberl D.D. & Jansen E. 2006. The Holocene history of drift ice in the northern North Atlantic: evidence for different spatial and temporal modes. *Palaeoceanography 21*, PA2017, doi: 10.1029/2005PA001214.

Mortensen A.K., Biglier M., Grönvold K., Steffensen J.P. & Johnsen S.J. 2005. Volcanic ash layers from the last glacial termination in the NGRIP ice core. *Journal of Quaternary Science 20*, 209–220.

O'Connor H.H. & Chang W.J. 1986. The amorphous character and particle size distributions of powders produced with the mirconizing mill for quantitative x-ray powder diffractometry. *X-ray Spectometry 15*, 267–270.

Olafsdóttir S. 2004. *Currents and climate on the northwest shelf of Iceland during the deglaciation: high-resolution foraminiferal research*. MSc thesis, Dept. of Geosciences, University of Iceland.

Oman L., Robock A., Stenchikov G.L., Schmidt G.A. & Ruedy R. 2005. Climatic response to high-latitude volcanic eruptions. *Journal of Geophysical Research—Atmospheres 110*, D13103, doi: 10.1029/2004JD005487.

Omotoso O., McCarty D.K., Hillier S. & Kleeberg R. 2006. Some successful approaches to quantitative mineral analysis as revealed by the 3rd Reynolds Cup contest. *Clays and Clay Minerals 54*, 748–760.

Pilcher J., Bradley R.S., Francus P. & Anderson L. 2005. A Holocene tephra record from the Lofoten Islands, Arctic Norway. *Boreas 34*, 136–156.

Prospero J.M., Bullard J.E. & Hodgkins R. 2012. High-latitude dust over the North Atlantic: inputs from Icelandic proglacial dust storms. *Science 335*, 1078–1082.

Pyne-O'Donnell S.D.F., Blockley S.P.E., Turney C.S.M. & Lowe J.J. 2008. Distal volcanic ash layers in the Lateglacial Interstadial (GI-1): problems of stratigraphic discrimination. *Quaternary Science Reviews 27*, 72–84.

Quillmann U., Andrews J.T. & Jennings A.E. 2009. *Radiocarbon Date List XI: East Greenland shelf, West Greenland Shelf, Labrador Sea. Baffin Island shelf, Baffin Bay, Nares Strait, and southwest to northwest Icelandic shelf. INSTAAR Occasional Paper No. 59*. Boulder: University of Colorado.

Rasmussen T.L., Wastegård S., Kuijpers A., van Weering T.C.E., Heinemeier J. & Thomsen E. 2003. Stratigraphy and distribution of tephra layers in marine sediment cores from the Faeroe Islands, North Atlantic. *Marine Geology 199*, 263–277.

Robinson S.D. 2001. Extending the distribution of White River ash distribution, northwestern Canada. *Arctic 54*, 157–161.

Sjerup H.-P., Lehman S., Haflidason H., Noone D., Muschler R., Berstad I.M. & Andrews J.T. 2010. Response of Norwegian Sea temperature to solar forcing since 1000 AD. *Journal of Geophysical Research—Oceans 115*, C12034, doi: 10.1029/2010jc006264.

Smith L.M. & Licht K.J. 2000. *Radiocarbon Date List IX: Antarctica, Arctic Ocean, and the northern North Atlantic. INSTAAR Occasional Paper No. 54*. Boulder: University of Colorado.

Stuiver M., Reimer P.J., Bard E., Beck J.W., Hughen K.A., Kromer B., McCormack F.G., van der Plicht J. & Spurk M. 1998. INTCAL98 radiocarbon age calibration 24,000-0 cal BP. *Radiocarbon 40*, 1041–1083.

Thompson R., Bloemendal J., Dearing J.A., Oldfield F., Rummery T.A., Stober J.C. & Turner G.M. 1980. Environmental applications of magnetic measurements. *Science 207*, 481–486.

Thompson R., Bradshaw R.W.H. & Whitley J.E. 1986. The distribution of ash in Icelandic lake sediments and the relative importance of mixing and erosiuonal processes. *Journal of Quaternary Science 1*, 3–11.

Thornalley D.J.R., Barker S., Broecker W.S., Elderfield H. & McCave I.N. 2011. The deglacial evolution of North Atlantic deep convection. *Science 331*, 202–205.

Till R. 1974. *Statistical methods for the Earth scientist*. New York: John Wiley & Sons.

Turney C.S.M., Harkness D.D. & Lowe J.J. 1997. The use of microtephra horizons to correlate Late-glacial lake sediment successions in Scotland. *Journal of Quaternary Science 12*, 525–531.

van den Bogaard C. & Schmincke H.-U. 2002. Linking the North Atlantic to central Europe: a high-resolution Holocene tephrochronological record from northern Germany. *Journal of Quaternary Science 17*, 3–20.

Wastegård S. & Davies S.M. 2009. An overview of distal tephrachronology in northern Europe during the last 1000 years. *The Holocene 24*, 500–512.

Wastegård S., Rundgren M., Schoning K., Andersson S., Björck S., Borgmark A. & Possnert G. 2008. Age, gechemistry and distribution of the mid-Holocene Hekla-S/Kebister tephra. *The Holocene 18*, 539–549.

Zhong Y., Miller G.H., Otto-Bliesner B.L., Holland M.M., Bailey D.A., Schneider D.P. & Geirsdottir A. 2011. Centennial-scale climate change from decadally-paced explosive volcanism: a coupled sea ice–ocean mechanism. *Climate Dynamics 37*, 2373–2387.